Bioinspired Surfaces with Dynamic Topography for Active Control of Biofouling

Phanindhar Shivapooja, Qiming Wang, Beatriz Orihuela, Daniel Rittschof, Gabriel P. López, and Xuanhe Zhao**

Biofouling, the accumulation of biomolecules, cells, organisms, and their deposits on submerged and implanted surfaces, is a ubiquitous problem across many human endeavors including maritime operations, medicine, food industries, and biotechnology.[1–3] Examples include: (i) the high cost of mitigation of biofouling on maritime vessels,[4] (ii) the growing significance of infectious biofilms (matrix-enclosed microbial adlayers) as a failure mode of implanted materials and devices,[1] and (iii) the adaptation of antibiotic-resistant bacterial strains within biofilms in medical and industrial settings.[5] Creating environmentally friendly and biocompatible surfaces that can effectively manage biofouling has been an extremely challenging "holy grail". In spite of substantial research efforts for several decades, cost effective control of biofouling is still an elusive goal in all areas that require long-term compatibility with biological systems.[2] Current commercial antifouling approaches and technologies include self-polishing surfaces that rely on controlled release of biocides[6,7] and fouling-release surfaces.[8] The next generation of fouling management includes specialized surface chemistries[9] and topographic patterns[10] that deter settlement of biofouling organisms. These approaches are generally limited to specific organisms or levels of fouling[1,3,4,9,11] and may have unacceptable impacts on the environment or human health with long-term usage.[7]

Nature offers multipronged solutions to biofouling that have not been implemented by humans.[12] An enormous number of biological surfaces clean themselves through active deformation and motion.[12–15] For example, cilia on the surfaces of respiratory tracts constantly sweep out inhaled foreign particles that are sequestered in hydrated, protective mucus layers.[13,14] Mucus sloughing and ciliary cleaning is also widely used by mollusks, corals and many other marine organisms for active fouling management.[12,15] Engineering surfaces coated with pillars that mimic cilia have been fabricated and proposed for biofouling management.[14,16] Despite their potential, surfaces coated with biomimetic cilia: (i) generally require complicated fabrication processes and are thus limited to relatively small areas, (ii) still require development of practical actuation schemes, and (iii) are made of fragile structures not suitable for harsh biofouling environments.

Here, we report a general, bio-inspired approach for actively and effectively detaching micro- and macro-fouling organisms through dynamic change of surface area and topology of elastomers in response to external stimuli. These dynamic surfaces can be fabricated from materials that are already commonly used in marine coatings and medical devices and can be actuated by practical electrical and pneumatic stimuli. New antifouling strategies based on active surface deformation can also be used in combination with other existing and emerging management approaches.

Figure 1a illustrates the structure of an electro-active antifouling coating (see Experimental Section for details of fabrication). Films of a silicone elastomer, a rigid insulating substrate, and a metal foil were bonded together to form a trilayer laminate.[17] The laminate can be readily fabricated to cover large areas. The elastomer surfaces were exposed to artificial-seawater suspensions of a model marine bacterium, *Cobetia marina* (7×10^7 cells/mL), which is known to colonize many materials rapidly and to modulate the attachment of other fouling organisms in seawater.[18] The *Cobetia marina* was allowed to form biofilms on the elastomer surfaces for 4 days (Figure 1a). The elastomer surfaces were electrically grounded by placing a ground electrode into the artificial seawater, which flowed gently over the surface of the attached biofilm. Control studies showed that the flow alone does not detach biofilms (see Figure S1 of the Supporting Information (SI)). As a DC voltage was applied to the metal foil under the laminate, an electric field developed in the elastomer. When the electric field exceeds a critical value, the surface of the elastomer becomes unstable, deforming into a pattern of "craters" (Figures 1a and b). The critical electric field for the electro-cratering instability can be expressed as[17]

$$E_c \approx 1.5\sqrt{\mu/\varepsilon} \quad (1)$$

where μ and ε are the shear modulus and dielectric constant of the elastomer. When the electric field is removed, the elastomer returns to its initial, flat topography. We characterized the surface strain of the elastomer under electric fields by imprinting

P. Shivapooja,[+] Dr. G. P. López
Department of Biomedical Engineering
Duke University
Durham, NC 27708, USA
E-mail: gabriel.lopez@duke.edu
Q. Wang,[+] Dr. G. P. López, Dr. X. Zhao
Department of Mechanical Engineering and Materials Science
Duke University
Durham, NC 27708, USA
E-mail: xuanhe.zhao@duke.edu
B. Orihuela, Dr. D. Rittschof
Duke University Marine Laboratory
Beaufort, NC 28516, USA
Dr. G. P. López, Dr. X. Zhao
Research Triangle MRSEC
Duke University
Durham, NC 27708, USA
[+] These authors contributed equally to this work.

DOI: 10.1002/adma.201203374

ADVANCED MATERIALS
www.advmat.de

www.MaterialsViews.com

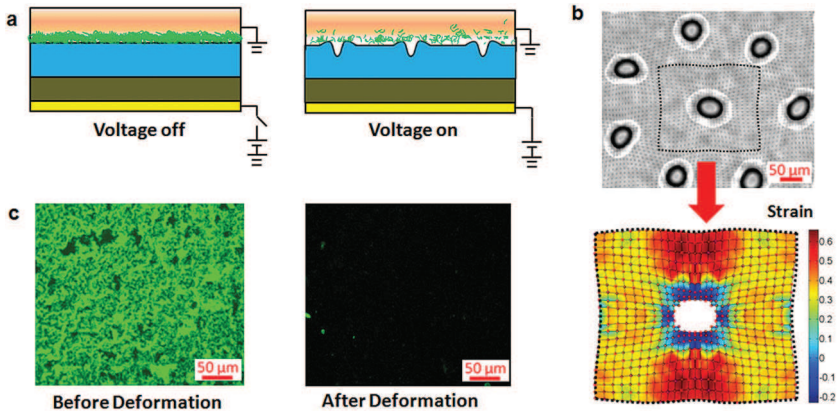

Figure 1. Detachment of bacterial biofilms from dielectric elastomers under voltages. a) Schematic illustration of the laminate structure, actuation mechanism, and the detachment of a bacterial biofilm. b) The applied electric field can induce significant deformation of the elastomer surface as given by the contours of the maximum principal strain. c) The deformation detaches over 95% of a biofilm (*Cobetia marina*) adhered to the elastomer surface, which is periodically actuated for 200 cycles within 10 minutes.

markers on its surface (Figure 1b). The size of the markers is much smaller than that of the craters and the markers form a regular square lattice on the undeformed surface. The surface strain is calculated by tracking the relative displacements of the markers (see Figure S2 of the SI). Figure 1b gives the distribution of the maximum principal strain on the deformed surface. It can be seen that the maximum principal strain is over 20% on most of the surface. After 200 on-off cycles of the applied voltage in 10 min, over 95% of the biofilm on the elastomer surface is detached (Figure 1c). To our knowledge, this is the first observation that voltage-induced deformation of polymer surfaces can actively and effectively detach adherent biofilms.

We hypothesized that the deformation of the elastomer surface, but not the presence of the electric voltage, causes biofilm detachment. To test this hypothesis, we decoupled the effects of the voltage and surface deformation on biofilm detachment using a set of silicone elastomer layers with moduli ranging from 60 kPa to 365 kPa. Biofilms of *Cobetia marina* were grown on the elastomer surfaces as described above. The applied electric fields in the elastomers were controlled according to Equation (1), such that the same electric field E can induce significant deformation for those elastomers where $E > E_c$ but not for those where $E < E_c$. In **Table 1**, the undeformed surfaces are indicated in italic text; significant detachment of biofilms (*i.e.* >85%) occurs only on those surfaces that undergo deformation. Although they were subjected to the same electric fields, the undeformed surfaces exhibited minimal detachment (*i.e.* <15%) of biofilms. These results support the assertion that surface deformation is the dominant mechanism for detachment of biofilms from the elastomer surfaces actuated by electric fields.

Next we studied the effect of surface deformation on the detachment of various forms of biofouling by mechanically stretching elastomers without imposition of electric voltages. Biofilms of different thicknesses on the elastomers were formed from *Cobetia marina* and *Escherichia coli* by varying their time in culture.[19] Then, each elastomer with biofilm was stretched uniaxially to a prescribed strain for 30 cycles within 3 minutes, while artificial seawater was gently flushed across the surface of the elastomer to carry away detached biofilm. After stretching, the percentage of biofilm detachment was measured as a function of the applied strain. **Figures 2**c,d show that surface deformation induces significant detachment of *Cobetia marina* and *Escherichia coli* biofilms (i.e., >80%) when the applied strain exceeds critical values ranging from 2% to 14%. The critical value of the applied strain depends on the thickness of the biofilm (Figure 2c). Interestingly, a thicker biofilm requires a lower critical strain for significant detachment.

We interpret the detachment of biofilms as a debonding process from the substrate.[20] Prior to debonding, the mechanical strain in the polymer layer and the biofilm is the same. If the biofilm is considered to be linearly elastic at the deformation rates used in the current study,[21] the elastic energy per unit area in the biofilm can be expressed as $HY^2_e/2$, where e is the applied strain, Y is the plane-strain Young's modulus of the biofilm, and H the thickness of the biofilm. Given that the biofilm maintains integrity over a length scale much larger than its thickness (See Figure S3 of the SI), debonding occurs when the elastic energy of the biofilm exceeds the adhesion energy between biofilm and the polymer. Therefore, the critical applied strain for the detachment of biofilm can be expressed as

$$e_c = \sqrt{\frac{2\Gamma}{HY}} \tag{2}$$

where Γ is the biofilm-polymer adhesion energy per unit area. Equation (2) predicts that the critical strain is a monotonically decreasing function of the biofilm thickness. The prediction is

Table 1. The percentage of *Cobetia marina* biofilm detached (%) from elastomer films (Sylgard 184) with various moduli and under a range of applied electric fields. The crosslinker density of the Sylgard 184 was varied to obtain elastomer films with shear moduli ranging from ~60 to 365 kPa. The electric field was periodically varied between zero and a maximum value (as shown in the table) for 200 cycles in 10 minutes. Imposition of electric fields below E_c caused no surface deformation (indicated by Italic text) and had minimal percentage (~15%) of biofilm detached. Imposition of electric fields below E_c resulted in formation of craters such that the surface switched reversibly from a flat state to the deformed state (indicated by normal text), resulting in high percentage (~95%) of biofilm detachment.

Electric Field [10 mV m^{-1}]	Shear Modulus [MPa]		
	0.060	0.155	0.365
2.3	12 ± 2.3	10 ± 2.5	11 ± 2
4.2	87 ± 7.1	15 ± 1.7	16 ± 5.5
7.0	88 ± 6	95 ± 2.7	11 ± 1.3
11.7	90 ± 3.6	96 ± 2.8	97 ± 1.6

DOI: 10.1002/adma.201203374

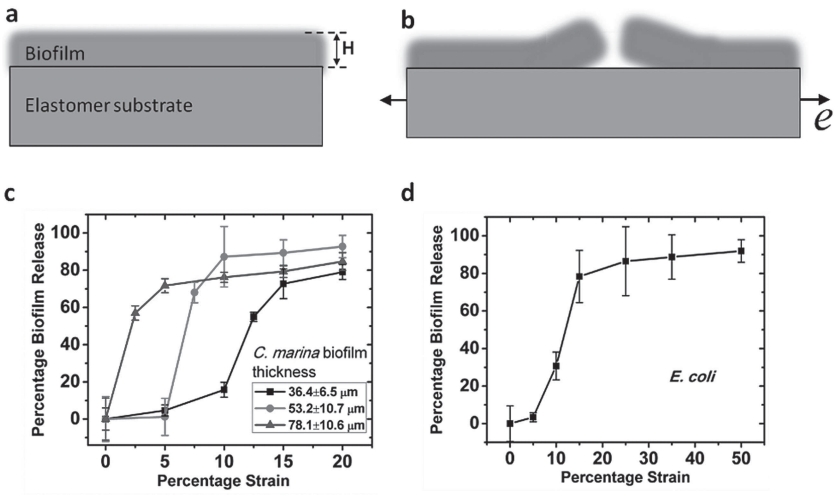

Figure 2. Debonding of biofilms from stretched elastomer films. a) Schematic illustration of the debonding mechanism. b) Percentage of detachment of *Cobetia marina* biofilm as a function of the applied strain. c) Percentage of detachment of *Escherichia coli* biofilm as a function of the applied strain. The elastomers are periodically stretched uniaxially to a prescribed strain for 30 cycles within 3 minutes.

consistent with the experimental results in Figure 2c, where a thinner biofilm requires a higher critical strain for the detachment.

To examine the effect of surface deformation on macrofouling organisms, we reattached adult barnacles, *Amphibalanus (= Balanus) amphitrite*,[22] to the surfaces of two types of silicone elastomers, Sylgard 184 and Ecoflex (**Figure 3**a, see SI for details). After the barnacles were reattached for 7 days, the elastomer layers were stretched to various prescribed strains periodically and then the shear forces for detaching the barnacles were determined.[22] The shear force for barnacle detachment was plotted as a function of the applied strain on the elastomer layer (Figure 3c). Deformation of the polymer significantly reduced the shear force required for barnacle detachment. For instance, an applied strain of 25% on the Sylgard 184 substrate (μ_s = 155 kPa) reduced the detachment force by 63%, and an applied strain of 100% fully detached the barnacles.

The debonding process of a barnacle due to substrate deformation can be understood as the symmetric propagation of two cracks at the barnacle–polymer interface (Figure 3b). The cracks propagate if the decrease of the elastic energy of barnacle–polymer system exceeds the adhesion energy between barnacle and polymer substrate.[23] The base plate of the barnacle is much more rigid than the polymer substrate.[24] The substrate under a row of barnacles (Figure 3c) is assumed to deform under a plane-strain condition (Figures 3a,b). The energy release rate due to crack propagation (i.e., the decrease of the system's elastic energy when the crack propagates a unit area) can be expressed as

$$G = \mu_s L f(e, L/S) \tag{3}$$

where μ_s is the shear modulus of the polymer substrate, L the length of the adhered region between barnacle and substrate, S the width of the substrate, and f a non-dimensional function given in Figure S4 of the SI by finite-element calculation. From Figure S4 of the SI, it can be seen that G is a monotonically increasing function of μ_s, e and L. By equating the energy

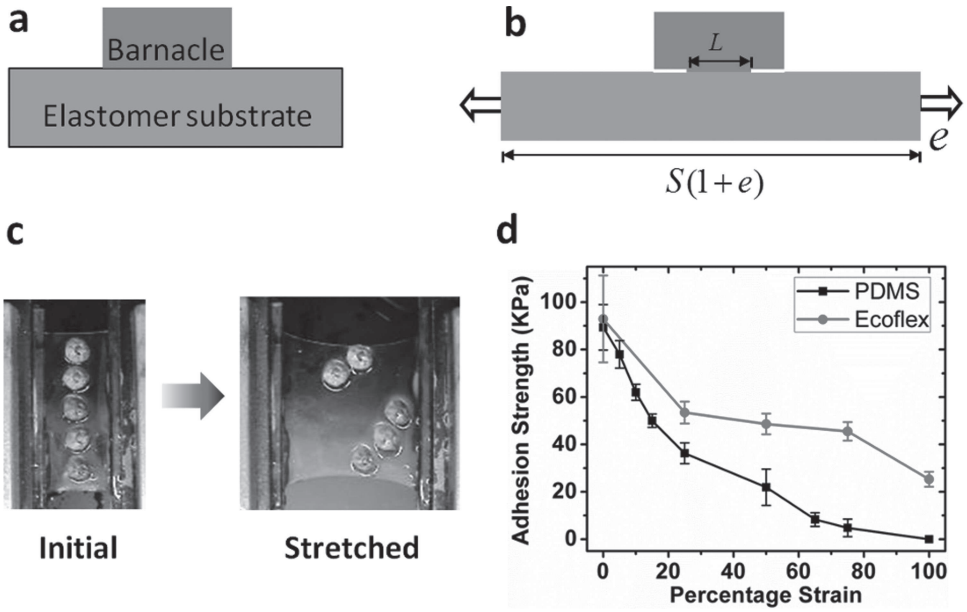

Figure 3. Debonding of barnacles from stretched elastomer films**.** a) Schematic illustration of the debonding mechanism. b) A photo showing the detachment of barnacles from a stretched elastomer film. c) The shear stress necessary to detach barnacles from the elastomer film decreases with the applied strain on the film. The elastomers are periodically stretched uniaxially to a prescribed strain for 30 cycles within 3 minutes.

ADVANCED MATERIALS
www.advmat.de

www.MaterialsViews.com

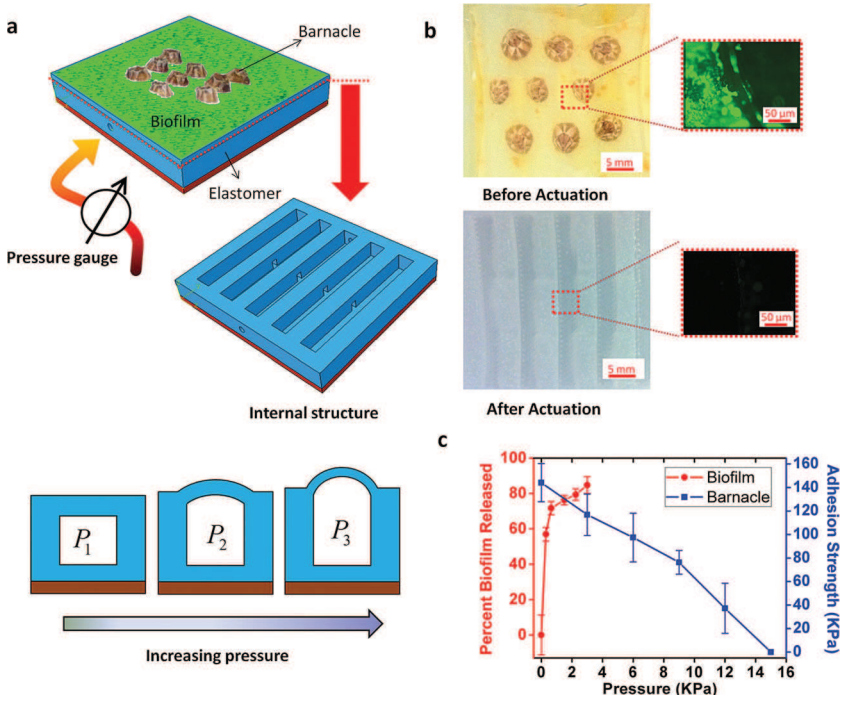

Figure 4. Detachment of bacterial biofilms from dynamic surfaces actuated by pressurized air. a) Schematic of the structure of the dynamic surface colonized by both a biofilm of *Cobetia marina* and barnacles, b) photos and fluorescent microscope images of the surface before and after actuation, and c) the percentage of biofilm detachment and the detachment shear stress for barnacles as functions of applied pressure. The dynamic surfaces are actuated for 30 cycles within 3 minutes.

release rate G with the adhesion energy between barnacle and substrate Γ, we can calculate the adhesion length L between barnacle and substrate at any applied strain e. From Figure 3d, the adhesion strengths for barnacle–Sylgard 184 and barnacle–Ecoflex systems are approximately the same. However, the Sylgard 184 (μ_s = 155 kPa) has a much higher shear modulus than the Ecoflex (μ_s = 10.4 kPa), and so, when subjected to the same applied strain, the Sylgard 184 substrate should detach barnacles more effectively (i.e. yield smaller L) than the Ecoflex substrate. This prediction is consistent with the experimental results (Figure 3d). Debonding of rigid islands from deformed substrates has been intensively studied theoretically[23,25] and experimentally[26] as a failure mode of electronic devices. Here, we demonstrated the debonding mechanism can be harnessed for active detachment of barnacles by deforming the substrates.

As an alternative means for achieving surface deformation, we examined the use of pneumatic networks[27] for active detachment of micro- and macro-biofouling models. As illustrated in **Figure 4**a, air channels were fabricated beneath an elastomer layer, while the bottom surface of the network was bonded to a rigid plate (see Figure S6 of the SI for details). When air is pumped into the channels, the top surface of the network buckles out and induces controlled surface deformation (Figure 4a). The relation between the air pressure and the strain of the surface is given in Figure S7 of the SI. Biofilms of *Cobetia marina* were grown on the surface of the elastomers for 7 days after adult barnacles were reattached to the surfaces and grown. The pressure in the air channels was gradually increased, and the coverage of biofilms and the shear stress for detaching barnacles were measured. As shown on Figure 4b and Figure 4c, the dynamic elastomer surfaces of the pneumatic network can actively and effectively detach both biofilms and barnacles. For example, an air pressure of 3 kPa induced 23% surface strain and almost 100% detachment of the biofilm. To fully detach the barnacles, a higher pressure (~15 kPa) was required. Soft robots[27] and snapping surfaces[28] driven by pressured air have been recently studied and proposed for a variety of applications. Here, we give the first demonstration of antifouling capabilities of dynamic surfaces actuated by pneumatic networks. We expect that hydraulic networks for deformation of elastomers[29] will perform similarly.

In summary, inspired by active biological surfaces, we created simple elastomer surfaces capable of dynamic deformation in response to external stimuli including electrical voltage, mechanical stretching, and air pressure. Deformation of polymer surfaces can effectively detach microbial biofilms and macro-fouling organisms. The use of dynamic surface deformation is complementary and can enhance other means for biofouling management such as surface modification, controlled release and micro- and nanotopography.

Experimental Section

Fabrication of electroactive surfaces: A rigid polymer substrate, Kapton, (DuPont, USA) with Young's modulus of 2.5 GPa and thickness of 125 μm was sputter-coated with a 10 nm gold layer underneath. A 50 μm polydimethyl siloxane (Sylgard 184 Dow Corning, USA) film, was spin coated on top of the Kapton film and cured at 65 °C for 12 hours. The crosslinker density of the Sylgard 184 was varied from 2% to 10% to obtain elastomer films with shear moduli ranging from 60 kPa to 365 kPa. The thickness and shear modulus of the films were measured by Dektak 150 Stylus Profiler (Bruker AXS, USA) and a uniaxial tensile tester (TA instruments, USA), respectively.

Formation of bacterial biofilms: *Cobetia marina* (basonym, *Halomonas marina*) (ATTC 4741) and *Escherichia coli* (ATTC 15222) in marine broth (MB) (2216, Difco, ATTC, USA) and trypsin soy broth broth (TSB), respectively, containing 20% glycerol were stored frozen in stock aliquots at –80 °C. Artificial seawater was prepared as reported previously.[6] Experimental stock preparations were maintained on agar slants and were stored at 4 °C for up to 2 weeks. A single colony from an agar slant was inoculated in MB (50 ml, for *Cobetia marina*) or TSB (50 ml, for *Escherichia coli*) and grown overnight with shaking at 25 °C (*Cobetia marina*) or 37 °C (*Escherichia coli*). The bacterial concentrations were 7×10^7 cells mL^{-1} and 11×10^7 cells mL^{-1} for *Cobetia marina* and *Escherichia coli*, respectively.

The surfaces used for growing biofilms were sterilized by rinsing several times with ethanol and then with copious amounts of sterilized DI water. *Cobetia marina* or *Escherichia coli* bacterial culture (1 mL) was placed on the sample surface along with sterilized artificial seawater or TSB broth (5 mL). The samples were stored for a desired period in an incubator maintained at 26 °C for *Cobetia marina* and 37 °C for *Escherichia coli*. The samples were carefully monitored, and artificial seawater or TSB

Adv. Mater. **2013**,
DOI: 10.1002/adma.201203374

broth (about 1 to 2 mL) was added as needed every day to compensate for dehydration. The thicknesses of biofilms were measured by inverted confocal microscope (Zeiss LSM 510) *(vide infra)*.

Barnacle reattachment on surfaces and adhesion strength measurements: Reattachment of barnacles followed a previously published protocol.[22] Briefly, barnacles (*Amphibalanus (= Balanus) amphitrite*) were reared to cyprids, settled on T2® (a gift from North Dakota State University) and cultured to a basal diameter of 0.5 cm in about 7 weeks. Barnacles were pushed off the T2 surface and immediately placed on the test surfaces in air and incubated in 100% humidity for 24 hours. Thereafter, the surfaces were submerged in running sea water and fed with brine shrimp daily for 2 weeks and tested.

Biofilm detachment from electroactive surface: A DC voltage was applied between artificial seawater and the bottom electrode by a controllable voltage supply (Mastsusada, Japan). The voltage was switched on and off at a frequency of 0.33 Hz for 10 minutes on each sample with a continuous low-shear flow (0.5 mL/min) of artificial seawater to carry away the detached biofilms. The electric fields shown in Table 1 were calculated using $E = \Phi/(h + H_s\varepsilon/\varepsilon_s)$, where Φ is the applied voltage, h is the thickness of Sylgard 184 film, $H_s = 125$ μm is the thickness of the substrate, $\varepsilon = 2.65\varepsilon_0$ and $\varepsilon_s = 3.5\varepsilon_0$ are the dielectric constants of Sylgard 184 and Kapton respectively, where $\varepsilon_0 = 8.85 \times 10^{-12}$ Fm^{-1} is the permittivity of vacuum.

Analysis of biofilm detachment: The biofilms on control and electroactuated samples were stained using SYTO 13 (Invitrogen Inc.); the procedure is detailed elsewhere.[30] The stain-washed biofilm surface was air dried in the dark for about 30 minutes and analyzed using a fluorescent microscope (Ziess Axio Observer) using a 10X objective. At least five images at different regions were captured from each stained surface under same exposure time. The average percentage of biofilm detached from the surfaces was calculated by comparing the relative fluorescence intensities between the experimental and control samples.

Biofilm and barnacle detachment from stretched surfaces: Films of the silicone elastomer, Ecoflex 00-10 (Smooth-On, USA) were used to detach biofilms or barnacles by mechanical stretching. The thickness and shear modulus of the Ecoflex films was 1 mm and 10.4 kPa, respectively. After biofilms and barnacles adhered to a film, the two ends of the film were clamped and stretched and relaxed in a periodic manner. The film was stretched to prescribed strains and relaxed for 30 cycles in 3 minutes, during which a continuous low-shear flow (0.5 mL/min) of artificial seawater was used to carry away the debonded organisms.

Fabrication of dynamic surfaces actuated by pressured air: As shown in Figure S6 of the SI, a plastic prototype fabricated in a 3D printer (Stratasys, USA) was used as a mold to cast an Ecoflex layer with patterned air-pass channels inside. The Ecoflex layer was then adhered to an uncured Ecoflex film (~200 μm) on a glass plate to bond the patterned Ecoflex layer with the glass plate.

Biofilm and barnacle detachment from dynamic surfaces actuated by air pressure: Barnacles were re-attached on the surfaces of Ecoflex layers and *Cobetia marina* biofilms were formed on the surfaces with barnacles for 6 days following the procedures described above. The Ecoflex layers were then actuated using a pneumatic pump (MasterFlex). By controlling the air pressure in the channels of the Ecoflex layers, the surfaces of the layer was reversibly deformed for 30 cycles in 3 minutes. The barnacle adhesion strength and the amount of biofilm released were analyzed following the procedure described above.

Supporting Information

Supporting Information is available from the Wiley Online Library or from the author.

Acknowledgements

The authors thank Linnea K. Ista and Leah Johnson for their technical assistance. The research is primarily supported by the National Science Foundation's Research Triangle Material Research Science and Engineering Center (DMR-1121107) and the Office of Naval Research (N00014-10-1-0907). X.Z. acknowledges the supports from NSF (CMMI-1200515) and NIH (UH2 TR000505). D.R. acknowledges the support from ONR (N00014-10-1-0850 and N00014-11-1-0180).

Received: August 15, 2012
Published online:

[1] L. Hall-Stoodley, J. W. Costerton, P. Stoodley, *Nat. Rev. Microbiol.* **2004**, *2*, 95.
[2] D. M. Yebra, S. Kiil, K. Dam-Johansen, *Prog. Org. Coat.* **2004**, *50*, 75.
[3] J. A. Callow, M. E. Callow, *Nat. Commun.* **2011**, *2*, 244.
[4] M. E. Callow, J. A. Callow, *Biologist (London)* **2002**, *49*, 10.
[5] J. D. Bryers, *Biotechnol. Bioeng.* **2008**, *100*, 1.
[6] L. K. Ista, V. H. Pérez-Luna, G. P. López, *Appl. Environ. Microbiol.* **1999**, *64*, 1603.
[7] K. V. Thomas, S. Brooks, *Biofouling* **2010**, *26*, 73.
[8] J. Y. Chung, M. K. Chaudhury, *J. Adhes.* **2005**, *81*, 1119.
[9] A. Rosenhahn, S. Schilp, H. J. Kreuzer, M. Grunze, *PCCP* **2010**, *12*, 4275.
[10] a) J. F. Schumacher, N. Aldred, M. E. Callow, J. A. Finlay, J. A. Callow, A. S. Clare, A. B. Brennan, *Biofouling* **2007**, *23*, 307; b) K. Efimenko, M. Rackaitis, E. Manias, A. Vaziri, L. Mahadevan, J. Genzer, *Nat. Mater.* **2005**, *4*, 293.
[11] a) R. F. Brady, *Prog. Org. Coat.* **1999**, *35*, 31; b) G. W. Swain, B. Kovach, A. Touzot, F. Casse, C. Kavanagh, *J. Ship Prod.* **2007**, *23*, 164.
[12] E. Ralston, G. Swain, *Bioinspir. Biomim.* **2009**, *4*, 1.
[13] a) A. Wanner, *Am. Rev. Respir. Dis.* **1977**, *116*, 73; b) H. Matsui, B. R. Grubb, R. Tarran, S. H. Randell, J. T. Gatzy, C. W. Davis, R. C. Boucher, *Cell* **1998**, *95*, 1005.
[14] T. Sanchez, D. Welch, D. Nicastro, Z. Dogic, *Science* **2011**, *333*, 456.
[15] M. Wahl, K. Kroger, M. Lenz, *Biofouling* **1998**, *12*, 205.
[16] a) B. A. Evans, A. R. Shields, R. L. Carroll, S. Washburn, M. R. Falvo, R. Superfine, *Nano Lett.* **2007**, *7*, 1428; b) R. Ghosh, G. A. Buxton, O. B. Usta, A. C. Balazs, A. Alexeev, *Langmuir* **2010**, *26*, 2963; c) P. Dayal, O. Kuksenok, A. Bhattacharya, A. C. Balazs, *J. Mater. Chem.* **2012**, *22*, 241; d) A. Sidorenko, T. Krupenkin, A. Taylor, P. Fratzl, J. Aizenberg, *Science* **2007**, *315*, 487.
[17] a) Q. Wang, M. Tahir, J. Zang, X. Zhao, *Adv. Mater.* **2012**, DOI: 10.1002/adma.201200272; b) Q. M. Wang, L. Zhang, X. H. Zhao, *Phys. Rev. Lett.* **2011**, *106*, 118301.
[18] a) J. S. Maki, D. Rittschof, M.-Q. Samuelsson, U. Szewzyk, A. B. Yule, S. Kjelleberg, J. D. Costlow, R. Mitchell, *Bull. Mar. Sci.* **1990**, *46*, 499; b) C. R. C. Unabia, M. G. Hadfield, *Marine Biol.* **1999**, *133*, 55; c) C. Shea, L. J. Lovelace, H. E. Smith-Somerville, *J. Microbiol. Biotechnol.* **1995**, 15.
[19] J. W. Costerton, Z. Lewandowski, D. E. Caldwell, D. R. Korber, H. M. Lappin-Scott, *Annu. Rev. Microbiol.* **1995**, *49*, 711.
[20] J. W. Hutchinson, Z. Suo, *Adv Appl. Mech.* **1992**, *29*, 63.
[21] T. Shaw, M. Winston, C. J. Rupp, I. Klapper, P. Stoodley, *Phys. Rev. Lett.* **2004**, 93.
[22] D. Rittschof, B. Orihuela, S. Stafslien, J. Daniels, D. Christianson, B. Chisholm, E. Holm, *Biofouling* **2008**, *24*, 1.
[23] N. Lu, J. Yoon, Z. Suo, *Int. J. Mater. Res.* **2007**, *98*, 717.
[24] D. B. Ramsay, G. H. Dickinson, B. Orihuela, D. Rittschof, K. J. Wahl, *Biofouling* **2008**, *24*, 109.
[25] S. H. Chen, H. J. Gao, *P. Roy. Soc. A-Math. Phy.* **2006**, *462*, 211.
[26] a) J. F. Waters, J. Kalow, H. Gao, P. R. Guduru, *J. Adhes.* **2012**, *88*, 134; b) J.-Y. Sun, N. Lu, J. Yoon, K.-H. Oh, Z. Suo, J. J. Vlassak, *J. Appl. Phys.* **2012**, 111.
[27] F. Ilievski, A. D. Mazzeo, R. E. Shepherd, X. Chen, G. M. Whitesides, *Angew. Chem. Int. Ed.* **2011**, *50*, 1890.
[28] D. P. Holmes, A. J. Crosby, *Adv. Mater.* **2007**, *19*, 3589.
[29] T. Thorsen, S. J. Maerkl, S. R. Quake, *Science* **2002**, *298*, 580.
[30] F. D'Souza, A. Bruin, R. Biersteker, G. Donnelly, J. Klijnstra, C. Rentrop, P. Willemsen, *J. Ind. Microbiol. Biotechnol.* **2010**, *37*, 363.

ADVANCED MATERIALS

Supporting Information

for *Adv. Mater.*, DOI: 10.1002/adma.201203374

Bioinspired Surfaces with Dynamic Topography for Active Control of Biofouling

Phanindhar Shivapooja, Qiming Wang, Beatriz Orihuela, Daniel Rittschof, Gabriel P. López, and Xuanhe Zhao**

Submitted to ADVANCED MATERIALS

Supporting Information

Bioinspired Surfaces with Dynamic Topography for Active Control of Biofouling

Phanindhar Shivapooja[†], *Qiming Wang*[†], *Beatriz Orihuela*, *Daniel Rittschof*, and *Gabriel P. López**, *Xuanhe Zhao**

[†] These authors contributed equally to this work.
*Email: gabriel.lopez@duke.edu; xuanhe.zhao@duke.edu

S1. Effect of shear flow alone on the detachment of biofilms

Biofilms formed on Sylgard 184 surfaces were subjected to a continuous flow of artificial sea water at 0.5 mL/min for 10 minutes as shown in **Figure S1a**. Analysis of the biofilm surfaces before and after flow did not show any significant detachment of the adhered biofilms as shown in **Figure S1b and c**. Thus, the flow was only able to remove the detached biofilm upon electro-actuation (**Figure 1**).

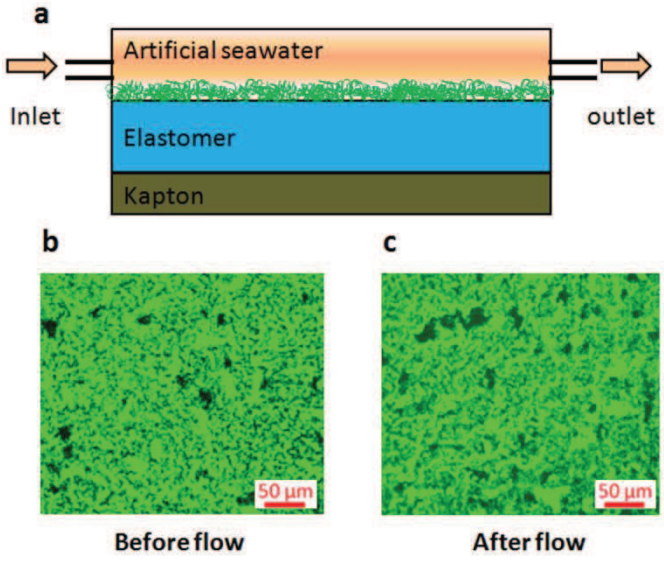

Figure S1. **Effect of the shear flow on detachment of biofilms.** (a) Schematic showing the flow on the *Cobetia marina* biofilm grown on Sylgard 184 for 6 days. Fluorescence images of the stained biofilm captured using 10 x objective (b) before flow and (c) after flow.

S2. Characterization of surface strain

The surface strain due to electro-actuation was characterized using markers imprinted on the surface. The fabrication procedure for the surface with markers is shown in **Figure S2a**. In brief, the markers were fabricated by casting a 50 μm thick Sylgard 184 film on a silicon mold with pillars arranged in a square lattice generated with photolithography. The feature size of the pillars on the mold is represented in **Figure S2a**. The distance between two adjacent pillars (5 μm) is much smaller than the thickness (50 μm) of the Sylgard 184 film. Therefore, the markers have negligible effect on the deformation of the Sylgard 184 film. Images (shown in **Figure S2b**) of the Sylgard 184 surface at flat and deformed states were captured by a microscope (Nikon, Japan). The initial (X_J) and deformed coordinates (x_i) were measured with an image processing software (ImageJ, NIH, USA) and the deformation gradient $F_{iJ} = \partial x_i / \partial X_J$ was computed using finite element analysis [31]. The Green strain was then calculated as $E = \left(F^T F - I\right)/2$, where I denotes the Kronecker delta tensor. The maximum principal Green strain was computed and plotted in Figure 1b.

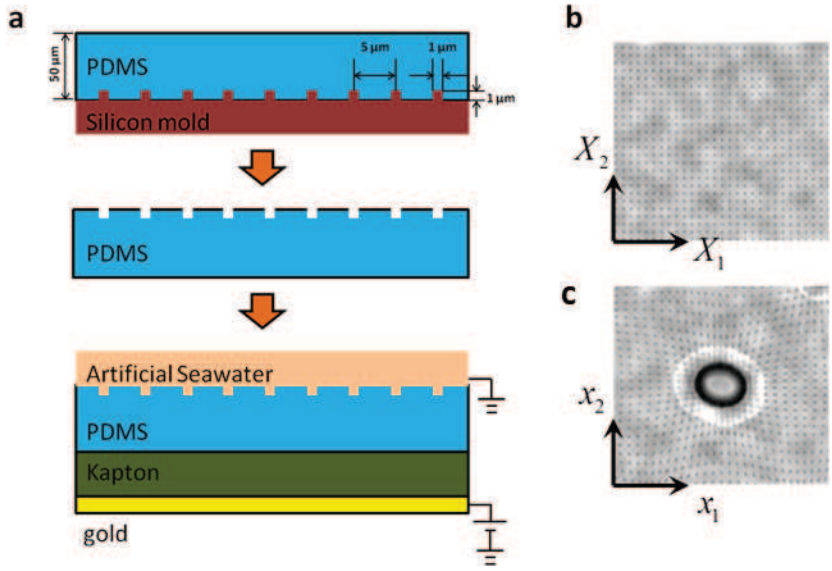

Figure S2. Surface deformation due to electro-actuation. (a) Schematic illustration of process for fabrication of the Sylgard 184 surface with markers. Phase contrast optical microscopy images of the Sylgard 184 surface in the undeformed, flat state (b) and the deformed, "cratered" state (c).

S3. Biofilm morphology on deformed substrate

Biofilms of *Cobetia marina* were grown on rectangular Ecoflex surfaces for six days and stained (see Methods). The stained biofilm gave a uniform coverage over most area of the Ecoflex surface as shown in **Figure S3a**. The Ecoflex substrate with the stained biofilm was then clamped on two opposing edges and slowly stretched in a uniaxial direction to 20% strain. The substrate was held in the stretched state and observed under the microscope to examine the effect of surface deformation on biofilm morphology. As shown in **Figure S3b**, the biofilms on the deformed substrate maintained its integrity over a length scale much larger than the thickness of the biofilms (i.e. 30 µm- 80 µm). Therefore, the detachment of the biofilm can be analyzed as a debonding process of a film from substrate.

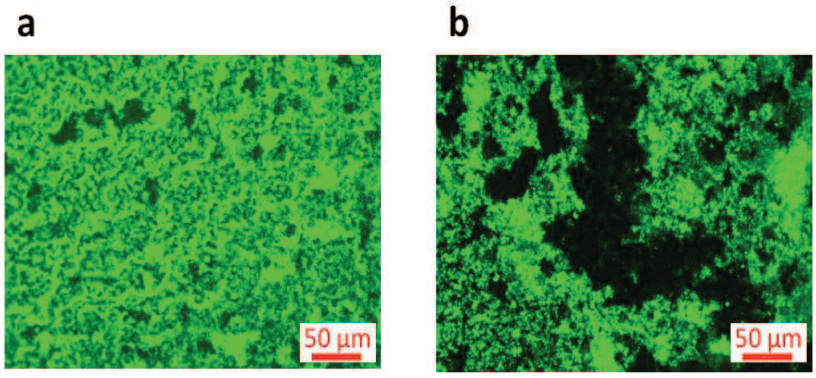

Figure S3. Fluorescence microscopy images of *Cobetia marina* biofilm surface before stretching (a) and after stretching to 20% strain (b).

S4. Energy release rate for debonding of barnacles.

The system of a row of barnacles on an elastomer film (**Figure 3c**) was simplified as a 2D plane-strain model as shown in **Figure S4a**. The Ecoflex film was modeled as a Neo-Hookean material with shear modulus μ_s and was assumed to be infinitely thick. The barnacle was modeled as a rigid body. The bonding length between the barnacle and the polymer substrate is denoted as L. The energy release rate G was computed by a commercial finite element package ABAQUS 6.10.1 (SIMULIA, USA). As shown in **Figure S4b**, the normalized energy release rate $G/(\mu_s L)$ increases with the applied strain e and the normalized contact length L/S, where S is the width of the polymer film. If the applied strain is small (e< 10%), the energy release rate can be analytically expressed as[32]

$$G = \frac{1}{2}\mu_s L\left[e^2 \tan\left(\frac{\pi L}{2S}\right)\left(\frac{S}{L}\right)\right] \qquad \text{(S1)}$$

In addition, if S is much larger than L, Equation (S1) further reduces to $G = \pi\mu_s L e^2/4$. From **Figure S4b**, it can be seen that the numerically calculated G at low values of e and L/S matches consistently with the analytical solution.

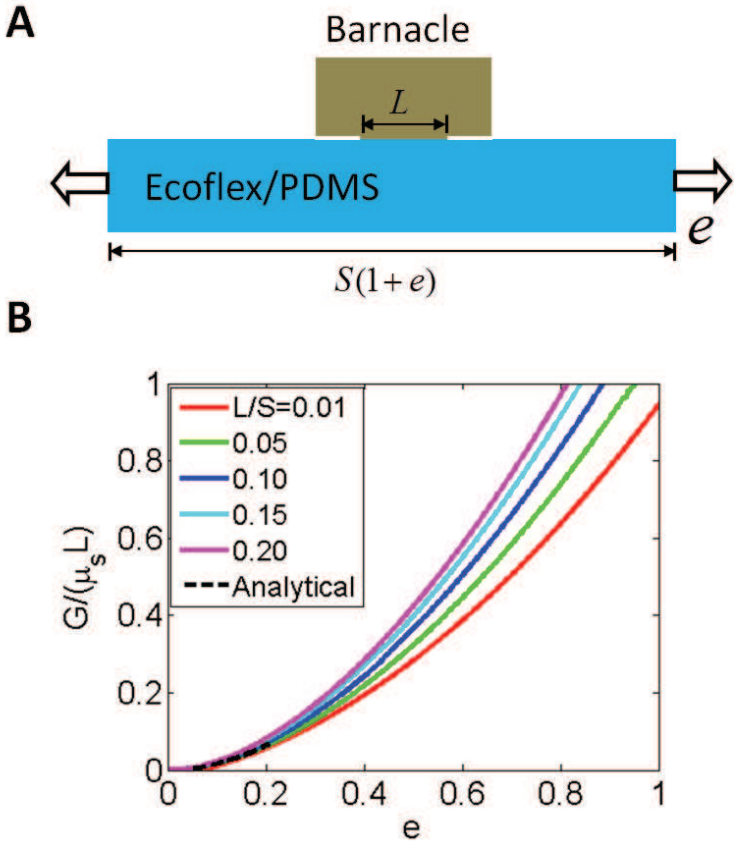

Figure S4. Normalized energy release rate for debonding of barnacle from the substrate. (a) Schematic for the elastomer-barnacle system under uniaxial stretching. (b) The relation between the normalized energy release rate with applied strain e and the ratio L/S.

S5. Biofilm thickness measurements

As shown in **Figure S5**, the thickness of the biofilm formed on the surface was measured using an inverted confocal microscope (Zeiss LSM 510) equipped with an argon ion laser operating at an excitation wavelength of 488 nm. For imaging, the biofilm was stained using SYTO 13 (see Methods). Using a 40X objective, a series of images were collected across the depth of the biofilm using the Z-stack software module provided by Zeiss. The start and end points for Z-stack imaging were determined by doing a fast XY scan while focusing on and out of the specimen surface; the images were automatically captured at each z-axis depth interval of 3 μm.

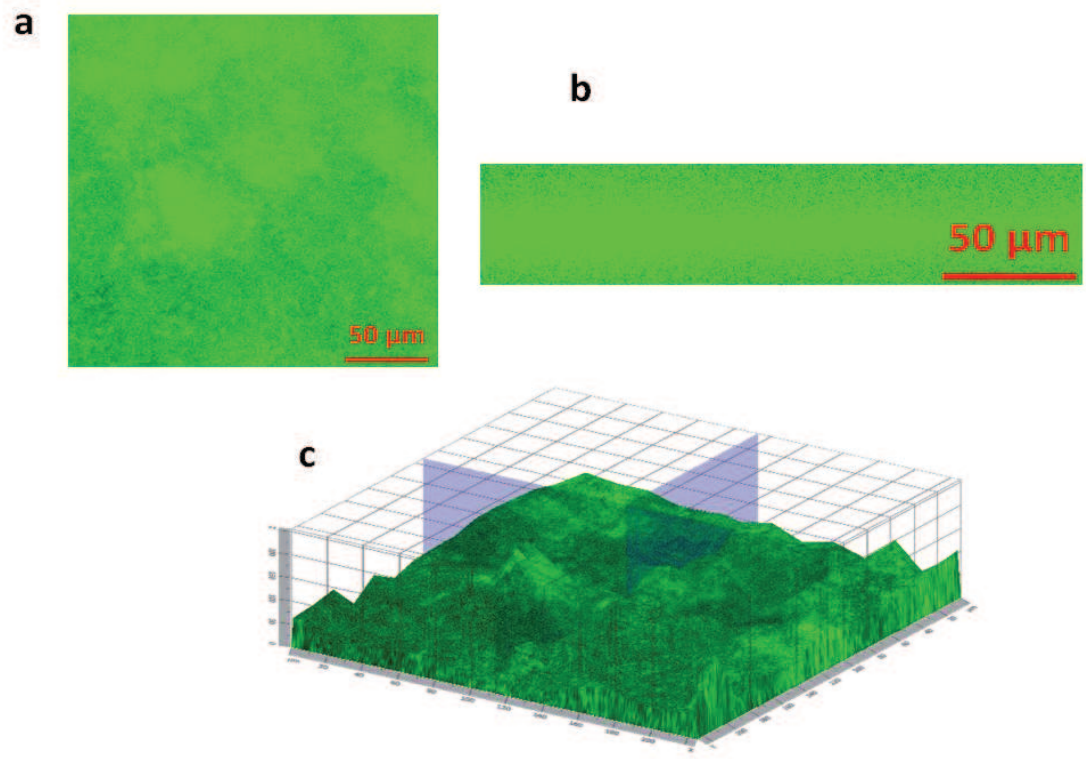

Figure S5. Confocal images of the Cobetia marina biofilm grown on Ecoflex for 4-days. (a) Z-stack image of *Cobetia marina* biofilm surface as seen from the top, (b) the cross-sectional view of the biofilm and (c) the 3-D reconstruction image of the biofilm.

S6. Process for fabrication of pressure-actuation prototype

As shown in **Figure S6**, a plastic prototype fabricated by a 3D printer (Stratasys, USA) was used as a mold to cast a patterned Ecoflex network. The network (**Figure S6b**) was then placed over an uncured Ecoflex film (~200 µm) spin-coated on a glass slide. After curing, the patterned Ecoflex network was firmly bonded to the glass slide to form enclosed air channels. Each air channel was covered by a long Ecoflex strips with thickness of ~1mm. Small holes were punched on two opposite walls of the network: one connected to a rubber tubing for air inlet and the other to a digital pressure transducer (Tachikara Inc.). As air pressure in the channels increases, the thin Ecoflex strip above the air channel buckles upward generating surface deformation.

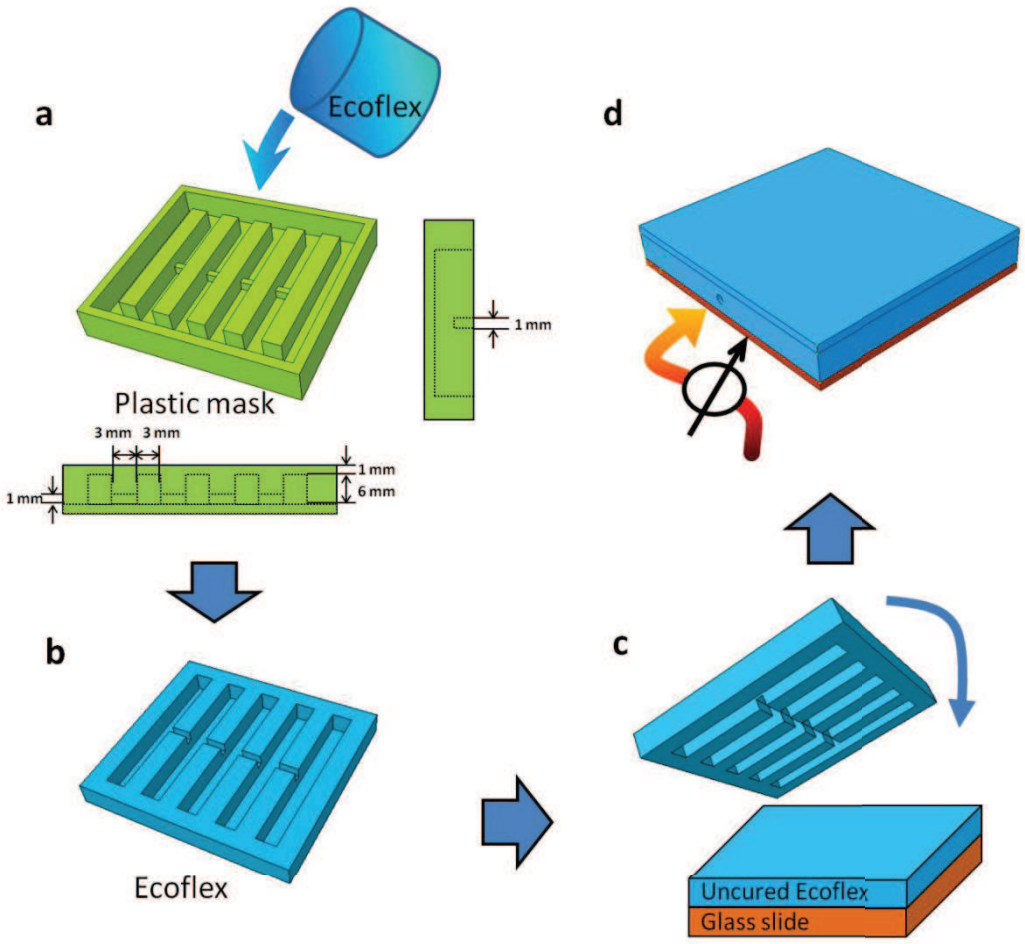

Figure S6. Fabrication of dynamic surfaces actuated by pressurized air. (a) A plastic prototype fabricated by a 3D printer was used as a mold to cast a patterned Ecoflex network. (b) Patterned Ecoflex with air-pass channels inside. (c) The patterned Ecoflex with air-pass channels inside was adhered on a glass slide with uncured Ecoflex. (d) After curing, the patterned Ecoflex with embedded air channels was firmly bonded to a glass slide.

S7. Pressure vs. strain for dynamic surfaces actuated by pressurized air

The pressure-controlled buckling of the Ecoflex strip above the air channel network was modeled as shown in **Figure S7a** [33]. A 2D plane-strain model was constructed to account for the deformation of the long Ecoflex strip. The Ecoflex strip clamped at two ends was subjected to a uniform pressure P, buckling out as an arc with radius R. We denote the initial

and blistered length as $2L$ and $2l$, and initial and blistered thickness of the film as H and h. As illustrated in **Figure S7a**, force balance gives

$$PR = \sigma_\theta h \tag{S2}$$

where σ_θ is the membrane stress. The two principal stretches in the film are

$$\lambda_\theta = \frac{l}{L} = \frac{\theta}{\sin\theta}, \quad \lambda_r = \frac{h}{H} = \frac{1}{\lambda_\theta} \tag{S3}$$

where 2θ is the angle of the arc as show in **Figure S7a**. The Ecoflex film obeys the Neo-Hookean model, i.e.

$$\sigma_\theta = \mu\lambda_\theta^2 - P_0, \;\; \sigma_r = \mu\lambda_r^2 - P_0 \tag{S4}$$

where P_0 is the hydrostatic pressure to ensure the imcompressibility of the elastomer. Given that the radial stress $\sigma_r \approx 0$, Equation (S4) gives

$$\sigma_\theta = \mu\left(\lambda_\theta^2 - \lambda_r^2\right) \tag{S5}$$

Combining Equations. (S2, S3, and S5), we can calculate the relation between the applied pressure P and the surface strain of the Ecoflex film $e = \lambda_\theta - 1$. The theoretical results consistently match with the experimental data (**Figure S7b**).

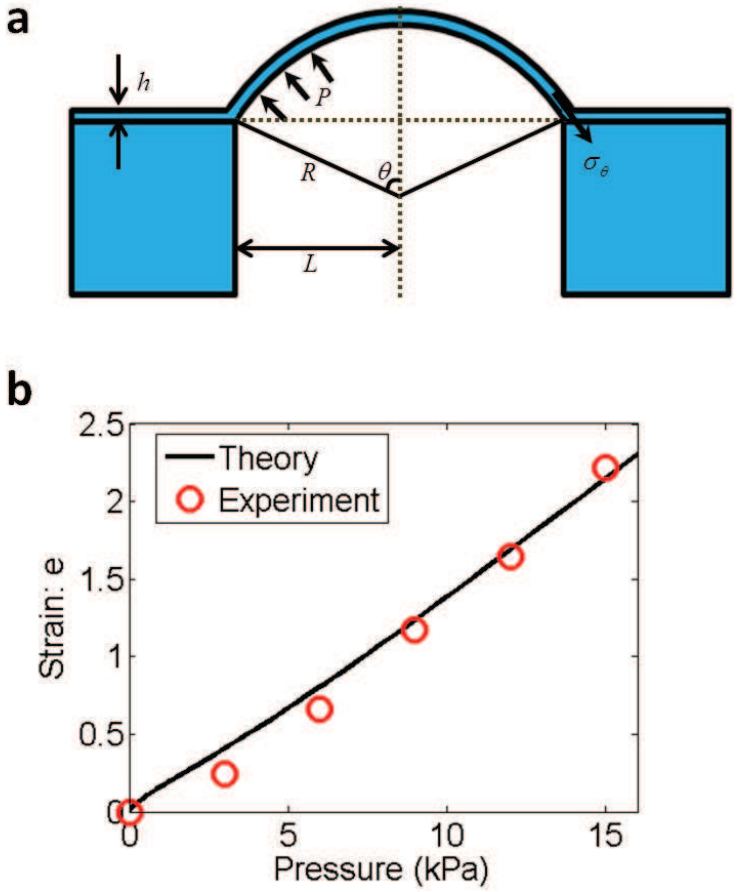

Figure S7. Pressure vs. strain for dynamic surfaces actuated by air pressure. (a) 2D schematic for blistering of the Ecoflex surface due to air pressure. (b) Relation between the surface strain and the air pressure.

Additional References

31. Hughes, T. J. R. *The finite element method: linear static and dynamic finite element analysis*. Vol. 65 (Dover Publications, 2000).
32. Lu, N., Yoon, J. & Suo, Z. Delamination of stiff islands patterned on stretchable substrates. *International Journal of Materials Research* **98**, 717-722, doi:10.3139/146.101529 (2007).
33. Williams, J. Energy release rates for the peeling of flexible membranes and the analysis of blister tests. *International Journal of Fracture* **87**, 265-288 (1997).